CHALLENGES IN THE MODELLING OF BLOWN CIRCULATION CONTROL AEROFOILS

Korbinian Stadlberger, Mirko Hornung
Institute of Aircraft Design, Technische Universität München, Germany

The present study contains a brief literature review that covers integral methods combined with potential theory as well as computational fluid dynamics mainly represented by RANS approaches. Own research efforts comprise the implementation of a Matlab tool whose environment provides an incompressible 2D RANS solver including Menter's k-ω-SST-model and Hellsten's stream line curvature correction. After a short description of the tool's main features the flow problem and its setup is specified and builds the basis of the performed numerical studies on lift generation. Comparing calculations with jet outflow through the upper slot confirm many of the uncertainties and difficulties found in literature when the RANS method is applied to model the diffusion-driven Coandă jet problem. While at low blowing rates the lift increments through trailing edge blowing agree sufficiently well for preliminary design purposes the results show significant difference for high blowing rates in the super-circulation region. A sudden rise in lift generation due to delayed jet detachment up to complete jet wrap around confirmed an instability in the RANS modelling method. Further numerical studies for dual-slot-blowing operation give hope for the applicability of this flow control concept for a flapless flight control effector system.

Nomenclature

α	global angle of attack
ΔC_d	increment of drag force coefficient
ΔC_l	increment of lift force coefficient
ΔC_m	increment of pitching moment coefficient
η	outflow momentum ratio in dual-slot-operation
ρ_∞	free stream air density
c	airfoil chord length
c_p	pressure coefficient
C_μ	blowing momentum coefficient
h	slot height
r	radius of Coandă surface
V_∞	free stream velocity
V_{jet}	mean jet exit velocity at slot

1 INTRODUCTION

In the framework of the national research program SAGITTA novel solutions for flapless flight control effectors are subject of investigation. In terms of low observability and maintenance cost it is of interest to avoid gaps between conventional flaps and to reduce the number of moving parts. The current study focuses on a circulation control concept that promises to meet requirements even beyond which particularly arise for low aspect ratio flying wing configurations [1]. This concept comprises active flow control at the rear fraction of an aerofoil by steady blowing over a blunt circular trailing edge (Fig.1). The jet flow over this round Coandă surface entrains the baseline airflow to the desired direction and thus manipulates the circulation strength. Basically a double-slotted trailing edge design acts similar to a conventional flap where the momentum vector is bended upwards or downwards (Fig.2). Additionally the current concept promises to be suitable also for yaw control when air flow momentum is controlled differentially on the wing half spans.

In order to evaluate the potential for control moment generation during all mission phases a global system model of the investigated concept is essential including pressurised air sources (e.g. engines), ducts and finally the control moment authorities through trailing edge blowing (Fig.3). The latter implies special challenges when computational efficiency and flexibility in terms of parameter variation is crucial for preliminary design stages. Even if vast amounts of fundamental wind tunnel experiments have been performed so far numerical modelling is still necessary to fill the gaps of missing

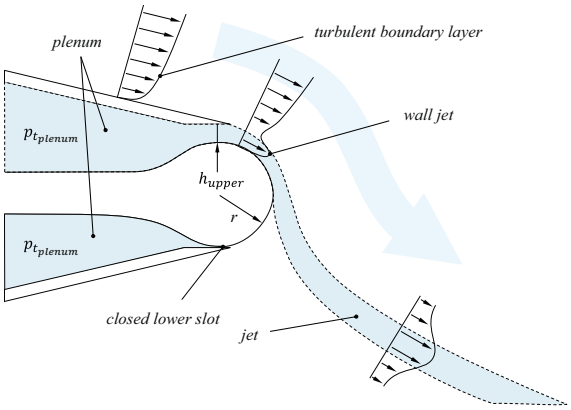

Fig. 1. Details of trailing edge flow (lower slot closed)

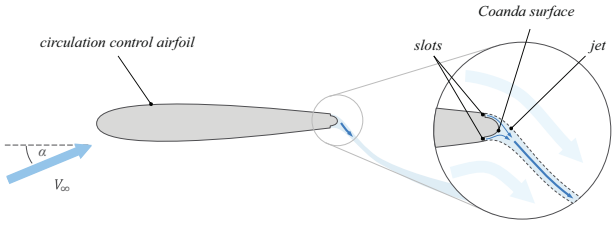

Fig. 2. Illustration of circulation control aerofoil in dual-slot-blowing operation

systematically collected data. The presented paper briefly summarises modelling attempts documented in literature from potential theory approaches to Direct Numerical Simulation (DNS). The subsequent sections describe the deduced flow problem and the in-house programmed Reynold's Averaged Navier-Stokes (RANS) simulation tool that is applied on reference cases from literature. The discussion of the numerical results finally points out raising issues during the validation of the applied simulation method.

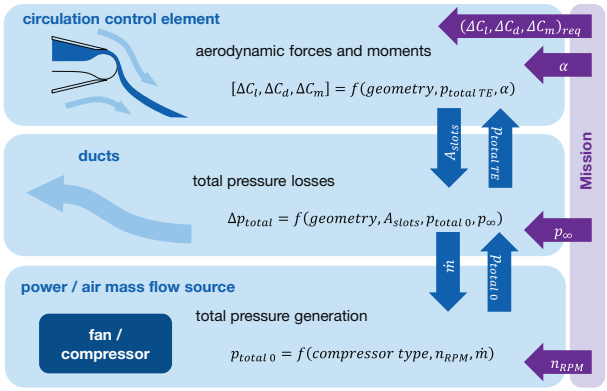

Fig. 3. Top level interactions of subsystem models

2 LITERATURE REVIEW

The following brief literature review focuses on modelling of the two-dimensional flow field around circulation control aerofoils with blown round trailing edges. Of course, at the end the control moment reactions of the entire flying wing configuration is of interest. However, recent experiments on finite wings gave indications that the conventional potential theory is applicable on circulation control wings [2, 3, 4] and section data can be translated into a finite wing. The impact of low aspect ratio was essentially the same as on conventional wings even if the spanwise flow component is potentially lower for circulation control wings. The modelling of 2D section flows in combination with extrapolation to the wing promises lower computational effort during automated calculation campaigns and higher robustness compared to fully three-dimensional CFD calculations.

The fundamental circulation control flow problem consists of a wall jet over a curved surface in adverse pressure gradient and is driven mainly by diffusion. The modelling of turbulence in the mixing layers is crucial as it is responsible for momentum transport into the viscous sublayer of the boundary layer on the Coandă surface and determines the separation point of the wall jet. The global impact of this rear stagnation point on circulation is massive and primarily section lift force as well as pitching moment vary strongly dependent on its prediction. The following subsections give examples of modelling attempts in the literature and underline the challenge of diffusion driven flow problems including separation phenomena, especially at high blowing rates. Starting with early attempts to model the Coandă effect with integral boundary layer methods and potential theory the second subsection finally summarises the most recent efforts to model circulation control aerofoils by use of the RANS approach.

2.1 Potential Theory and Integral Methods

Right at the beginning of intensive experimental research on circulation control technology in the 1960s simultaneous analytical modelling approaches have been applied on the wall jet behaviour along a curved Coandă surface [5, 6]. According to the potential theory practice a vortex superimposed on a doublet was used to describe the global flow field around

a tangentially blown cylinder in free stream. Then parametrised velocity profiles were prescribed both for laminar and turbulent regions on the windward surface that are unaffected by the wall jet. This enabled the application of an integral method to model the main characteristics of the well-known boundary layer shapes. A similar approach was chosen for the particular wall jet velocity profile which was divided into four layers [6] in order to solve the momentum equations analytically. This multi-strip integral method accounted for curvature effects that manifest itself in normal pressure gradients which are normally neglected in the standard boundary layer approximation. However, due to many approximations the calculation method still resulted in significant differences with experimental results, especially at higher jet momentum.

In the end of the 1970s the tested circulation control aerofoils were represented by a vortex lattice arrangement with additional source distribution to account for boundary layer thickness [7]. The boundary layer flow on the lower and the upper surface before the slot was calculated using integral methods that account for laminar and turbulent regions with transition point estimation. In the Coandă surface section from the slot to the jet separation point a finite difference technique of the Crank-Nicholson type estimated the jet flow behaviour and also considered normal pressure gradients. In order to model the turbulence a modified Van Driest eddy viscosity model was applied on the inner region of the jet while the outer region underlay a newly formulated eddy viscosity model [8] which additionally accounted for the effects of curvature. The iterative calculation process has converged when the upper and lower separation pressure on the Coandă surface both coincided within a prescribed tolerance. This program (CIRCON) was able to predict the jet separation as well as the aerofoil flow field quite accurately and achieved remarkable results. Later the calculation tool has been extended for transonic flow conditions, where both calculations of potential theory and boundary layer had to be adapted to account for compressibility effects [9]. Last modifications comprised the introduction of the curvature corrected k-ϵ turbulence model for the outer layer of the wall jet as well as modified solution strategies for increased Coandă surface contour sensitivity and supersonic wall jets [10].

2.2 Computational Fluid Dynamics

Turbulence measurements in the wind tunnel indicate that the external free stream plays an important role in the overall mixing of the different jet layers and with it also in the behaviour of the jet following the surface contour [11]. Therefore a segregated modelling approach of the wall jet without global flow field interaction might lead to favourably low computational efforts but does not reach the desired accuracy. Here, the solution of the momentum and conservation equations with turbulence closure for the entire aerofoil flow field in the two-dimensional case appears more promising even if computing times rise significantly. On this subject the following summary is intended to give a short overview of the most recent modelling activities and investigations in the field of numerical fluid dynamics.

Whereas some modelling efforts indicate a certain success in using RANS to predict trends and selected details there have been more failures of RANS models than successes. Failures typically manifest themselves in a wall jet which stays attached too long and leads to an excessive over prediction followed by a gross under prediction of the lift coefficient when the jet wraps around and deteriorates the lower pressure distribution [12, 13, 14, 15]. Here, tangential grid refinement at the Coandă surface can help but does not always cure the problem [16]. In addition, numerical results often underestimate the experimentally measured suction peak on the circular trailing edge. One cause is setting the momentum flux too low for the inflow boundary condition of the jet outflow, which results in a too low jet exit velocity that is often determined analytically by use of the plenum pressure ratio. Nevertheless, Baker and Paterson [17] could achieve remarkably good results, however, Swanson and Rumsey [16] claim that the effects of incompressible solver and not considered α-correction for sidewall effects compensate each other. The incompressible flow simulation of the transonic jet results in a lower acceleration of the jet flow than required but the nominal angle of attack instead of the effective α counterbalances the loss of circulation over most of the circulation control aerofoil. This solution of the ‘‘wrong problem” could be reproduced by Swanson and Rumsey [16]. Especially at higher blowing rates

and high lift generation interactions of the jet sheet with tunnel side walls can be crucial. They cause vortices downstream which induce a net downwash on the aerofoil and reduce the effective angle of attack significantly [18, 19, 20, 21, 22]. Furthermore, the turbulence model used for RANS closure is highly crucial for the final result, as the eddy viscosity predictions inside the wall jet determine the location of jet separation. Unfortunately a distinct all-embracing statement about the most appropriate turbulence model for circulation control is not possible if one has to give a final conclusion of available literature at present. It is of interest that the more complex full Reynold's stress model did not turn out to be superior either [15, 14], even if it is supposed to be theoretically more suitable for the wall jet problem due to its anisotropy [23]. Also the attempt to adjust the constant coefficients of the k-ω-turbulence model depending on the blowing case could not improve the predictability of a general design [24]. However, turbulence models with implemented flow curvature correction (e.g. Hellsten [25], Shur et al. [26]) tend to alleviate the problem of non-physical solutions at high blowing rates but give no guarantee [19, 13, 12, 27]. Moreover systematic calculations of Min et al. [28] indicate that the order of spatial discretisation has minor effect on the accuracy of the final results. Similarly the inclusion of the plenum chamber before the slot exit instead of simply assign the boundary conditions directly at the slot showed no significant impact. However, the lift performance revealed visibly sensitive to the prescription of turbulence level at the slot exit boundary. In addition, calculations performed by Nishino and Shariff [29] investigated the influence of jet nozzle lip thickness and underline the importance of turbulent processes in the region close to the slot. Their results showed that the jet profile across the nozzle exit is insensitive to the nozzle lip thickness, however, the jet flow downstream of the nozzle exit, i.e. the circulation around the aerofoil, is to some extent dependent on the lip thickness due to the varying momentum losses.

Finally, the increase of computational effort by performing Large-Eddy-Simulations (LES) [30] as well as Direct Numerical Simulation (DNS) [31] could not outperform the RANS methods in terms of prediction accuracy where deviations of the pressure distribution at high blowing rates still exist. As concluding remark the statement of Swanson and Rumsey [16] has to be extended at present: "the current prediction capability with numerical methods for circulation control flows over Coandă surfaces is not ready for a general design procedure", neither with RANS methods nor with LES or DNS approaches.

3 NUMERICAL STUDY

Next the used tool and the two-dimensional model setup are described before some results are presented containing the experiences made during validations with wind tunnel data from literature.

3.1 Methods and Implementation

The following subsections give an overview of the MATLAB tool including the underlying methods and implemented features.

3.1.1 Governing Equations and Discretisation

In order to reduce computational efforts and to increase robustness the fluid of the given flow problem is considered as an incompressible Newtonian fluid. Past numerical studies have shown negligible influence of compressibility for moderate jet exit velocities [27]. According to the finite volume method the incompressible momentum equations for a velocity component u_i in cartesian coordinates can be written in the following integral form by using Gauss's divergence theorem

$$\int_{CV} \frac{\partial (u_i)}{\partial t} dV + \int_A \vec{n} \cdot \left(u_i \cdot \vec{u} \right) dA = - \int_{CV} S_{p_i} dV + \int_A \vec{n} \cdot \left(\mu_{eff} \operatorname{grad} u_i \right) dA + \int_{CV} S_{u_i} dV \quad (1)$$

where $S_{p_i} = \frac{\partial p}{\partial x_i}$ constitutes the pressure source term and S_{u_i} an arbitrary momentum source term. The normal vectors on the control volume's (CV) boundary surfaces A are denoted by $\vec{n}$. In the implementation of the steady solver the transient terms $\int_{CV} \frac{\partial \Phi}{\partial t} dV$ were omitted.

The continuity equation is given by

$$\int_{CV} \frac{\partial \rho}{\partial t} dV + \int_A \vec{n} \cdot \vec{u} \, dA = 0 \quad (2)$$

The current implementation includes the hybrid differencing scheme which combines both upwind and central differencing scheme [32]. Depending on the local Peclet number the second-order accurate central differencing scheme or the unconditionally stable upwind differencing scheme is employed and prevents numerical instabilities due to coarse discretisation. In order to avoid a non-physical discretisation induced “checker-board” pressure field a staggered grid approach for velocity components and scalar parameters has been implemented [33].

3.1.2 Solver

For the estimation of attainable forces and moments in a two-dimensional case the steady incompressible Reynolds Averaged Navier-Stokes equations are solved in the MATLAB environment. As it is basically designed for matrix and vector operations it offers a lean syntax for nearly fail-safe code generation. The mathematical operations emerging from the discretisation and the treatment of the linearised partial differential equations belong to common mathematical procedures MATLAB was originally designed for. Even if the real-time code line processing leads to reduced computational performance it is optimised for matrix operations and additionally provides powerful debugging possibilities. All variables can be checked, modified and above all instantaneously processed by an experimentally differing line of code during runtime. Especially for two-dimensional problems the user-friendly variable explorer accelerates code development. Moreover the ability of MATLAB to handle sparse matrices provides user-friendly programming without excessive use of memory for fluid dynamic problems.

Similar to the commercial solver CFX from Ansys Inc. a coupled solver strategy has been chosen. Altogether momentum and continuity equations are solved simultaneously in one system of linear equations to compute velocities and pressure (u, v, ψ). Compared to segregated solver methodologies (e.g. SIMPLE(R,C), PISO etc.) the coupled approach reveals much more robust and needs fewer iterations to converge. However, the memory requirements increase considerably when flow domains with large cell numbers have to be solved. In the present application a standard personal computer provides enough memory ($\sim\ 4GB$) to calculate the two-dimensional flow domain with sufficient accuracy. MATLAB includes an ample library of regularly optimised built-in functions that help to treat common mathematical and geometrical problems in a naturally parallelised manner. During the iterative process the solution of the linear system of equations constitutes the main fraction in terms of computational cost. The corresponding function is based on FORTRAN subroutines (UMFPACK) that solves this step at high performance. Unfortunately it is only partially parallelised so that the full computational power of a cluster cannot be exploited yet.

3.1.3 Turbulence Model

As already mentioned in 2.2 the turbulence model is crucial for diffusion driven circulation control applications. In general, accuracy and computational effort have to be compromised by choosing a turbulence model that consists of a higher or lower number of equations to be solved. Since no clear superiority of a full Reynold’s stress model could be identified in terms of accuracy, Menter’s k-ω-model with shear stress transport (SST) [34] was selected to be implemented into the flow simulation tool. In the literature it produced satisfactory results over a quite large amount of references, even if its limits became visible at higher blowing rates as well. The implementation includes a correction for curved streamlines following the approach of Hellsten [25].

3.1.4 Automation

Several automated features have been implemented as the tool is intended to be used for large calculation campaigns on a Linux cluster system including widespread parameter variations. An automated mesher with algebraic initialisation and subsequent orthogonalisation through elliptic solver creates a grid on the basis of given baseline aerofoil coordinates, trailing edge radii and nominal slot heights. The aerofoil shapes of the NACA families can be retrieved automatically by means of an integrated external NASA tool (naca456). In order to increase robustness and convergence rate at the beginning of the iterative calculation process the flow field is initialised by an approximated inviscid solution evolving from potential theory. Discrete potential vortices and respective control points distributed along

the aerofoil contour represent the inviscid flow field that finally is determined by the Kutta condition at the trailing edge. A guessed angle sets the aft stagnation point on the Coandă surface which enables a fast solution of the system of linear equations for potential vortex strengths. Finally, an automated calculation campaign for several operation points can be launched after the free stream and blowing properties have been specified. At runtime problem specific flow phenomena as leading edge separation and jet wrap-around are detected and can be used to control the further proceedings of calculations. A convergence detection enables the premature completion of each single calculation leading to significant time savings.

3.2 Problem Outline

The flow problem consists of an aerofoil with a blunt trailing edge with radius r exposed to a free stream with velocity V_∞ and angle of attack α (Fig.2). The internal pressurised air with total pressure $p_{t_{plenum}}$ accelerates at the end of the plenum and leaves the slots with the respective heights h_{upper} and h_{lower} having a mean velocity V_{jet} (Fig.1). The wall bounded jet mixes with the turbulent boundary layer flow arriving from the upper side of the aerofoil and forms the typical wall jet velocity profile on the Coandă surface (Fig.1). Depending on the jet's turbulence characteristics and counterpressure arising from each other both wall jets separate and build one single jet in free stream. Further turbulent and viscous mixing processes alleviate the over velocities until complete free stream assimilation. As circulation increases with blowing rate a shift of leading edge stagnation point as well as an intensified suction peak with possible short separation bubble can be expected.

For the double-slotted circulation control aerofoil an O-grid mesh topology (Fig.4) was chosen as grid distortions and skewed cells are supposed to be reduced to a minimum. The aerofoil grids for the subsequent numerical studies have a total longitudinal point number of about 500 around the entire surface with approx. 100 of these points concentrated on the Coandă trailing edge. The grid section covering the wall jets has approx. 80 points in the normal direction to the surface where the total number of grid points was between 50,000 and 100,000 for the investigated meshes. The normal gird spacing inside the boundary layers was resolved

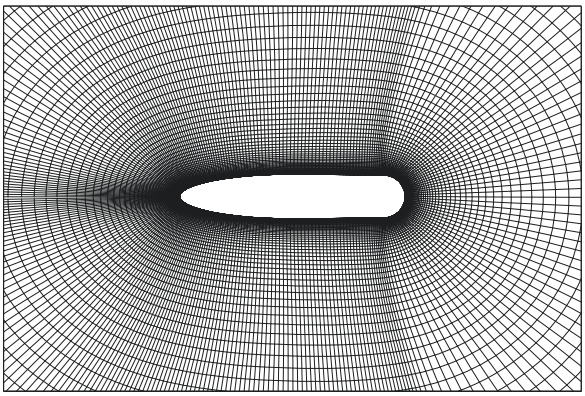

Fig. 4. Example of used mesh with O-grid topology

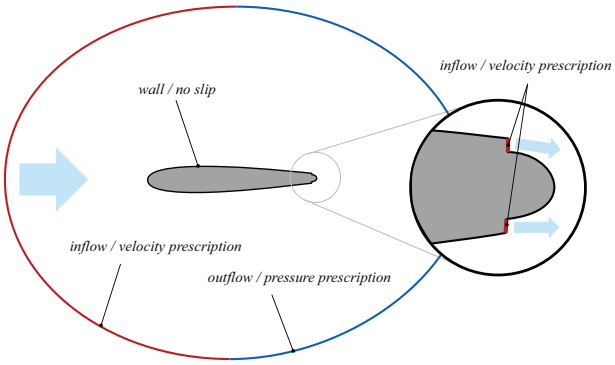

Fig. 5. Illustration of flow domain boundary conditions

such that the first grid points adjacent to the wall fulfil the requirement $y^+ < 1$. Test calculations with mesh refinement did not lead to significant differences in the scope of preliminary design stages that would justify the higher computational effort. A similarly low sensitivity was experienced in literature [16, 35, 36]. Finally the boundary conditions of the two-dimensional flow domain are set as illustrated in Fig.5 where the farfield boundaries are defined approximately 15 chord lengths distant from the aerofoil surface. The jet velocity profile at the slot inlets is defined by a power-law approximation which is introduced into empirical formulas for turbulent scalar estimation at the slot boundaries.

In the literature it is common to describe the force and moment reactions dependent on the normalised momentum flux of the outflow, i.e. the equivalent thrust force. The flow momentum coefficient C_μ therefore yields

$$C_\mu = \frac{\dot{m}_{jet} V_{jet}}{\frac{1}{2}\rho_\infty V_\infty^2 S_{ref}} \tag{3}$$

where $\dot{m}_{jet}$ is the jet mass flow, V_{jet} the jet outflow velocity, $\frac{1}{2}\rho_\infty V_\infty^2$ the free stream dynamic pressure and S_{ref} the lifting surface reference area.

3.3 Numerical Results

This study consists of the modelling of wind tunnel experiments on double-slotted circulation control aerofoils from two different sources (Table 1). After many years of research activities in the field of blown aerofoils Englar et al. at last published wind tunnel data in 2009 that was meant to depict a benchmark for validation purposes [21]. The symmetric semi-elliptical 20%-thick aerofoil is characterised by a relatively large radius of the trailing edge Coandă surface. Even if it is not representative for technical applications it simplifies the use of measurement equipment and enables detailed investigations of the processes inside the jet sheet. In 2005 Alexander et al. performed and published wind tunnel tests on a 6%-thin slightly cambered elliptical aerofoil whose equally elliptical trailing edge shape could be varied [37]. In principle, the latter aerofoil shape is closer to reasonable technical applications in aviation and was investigated in the form of a half wing with endplate up to transonic conditions. In this article the discussion is limited to the behaviour of the lift force reactions that have been predicted by own calculations. Overall pitching moments agreed sufficiently well when lift force was estimated correctly and drag predictions from RANS have to be handled with care anyway due to possible viscous effects that can hardly be modelled by the underlying method. The calculations in the scope of this study were performed on in-house desktop machines equipped with Intel Core i7-4770 processors (quad core à 3.40Ghz) and 8GB RAM. Depending on the grid size one iteration took between 5s and 15s where convergence was attained after 80 to 200 iterations in the majority of cases.

3.3.1 Unblown Aerofoil

For the extraction of the force and moment increments (ΔC_l, ΔC_d, ΔC_m) the reference values $(C_l,\ C_d\, C_{m,})_{V_{jet}=0}$ of the unblown aerofoil are crucial for flight control system evaluation. Wind tunnel experiments reveal that the Reynold's number has a significant effect on the lift curve slope of elliptical aerofoil sections [38]. At higher subsonic Reynolds numbers ($2 \cdot 10^6$) the lift curve slope

Table 1. Modelled double-slotted circulation control aerofoils

	Englar et al. [21], 2009	Alexander et al. [37], 2005
$\frac{t}{c}$	20%	6%
camber	0%	0.75%
$\frac{r}{c}$	0.095	$\backsim$ 0.025
$c\,[m]$	0.22	0.71
Re	$\backsim$ 500,000	$\backsim$ 1,000,000
$h_{slot}\,[mm]$	0.23, 0.33, 0.46, 0.66, 1.09	0.53, 0.89, 1.42, 1.85

falls below that of a conventional aerofoil as it may be expected due to separations at the trailing edge and the resulting thick wake layer. However, at low Reynold's numbers of about 300,000 the lift curve slopes can be much higher than 2π for low angles of attack as a consequence of early laminar separation from the lower side in combination with attached flow around nose and suction side. In case of a double-slotted aerofoil the separation point is assumed to be defined by the contour steps formed by the slot lips. In addition, these laminar effects disappear when early transition is provoked by boundary layer trips. Therefore fully turbulent RANS calculations are supposed to be accurate enough for modelling purposes in both cases. Fig.6 shows the reference curves and the corresponding results from RANS calculations. For reference Englar et al. the results agree well in the region of low angles of attack while the numerical model overestimates produced lift at higher angles of attack. Despite the boundary layer trip viscous flow separation effects seem to weaken the real lift curve slope early before stall. In contrast, for reference Alexander et al. the numerical results for $Re = 1,000,000$ agree quite well throughout the entire α range when the original experimental curve is corrected by an zero lift angle of attack $\alpha_0 = -1°$ as would be approximately predicted by common methods from literature [39]. Even if the modelled flow was characterised by short leading edge separation bubbles beginning at $\alpha = 5°$ the lift curve slope and maximum lift could be reproduced accurately enough for preliminary design requirements. In any case the circulation control potential near stall is no primary research objective.

3.3.2 Single-Slot-Blowing

In general, two different operating modes can be seen with increasing jet momentum ejected solely through the upper slot. Initially, the device is a very effective

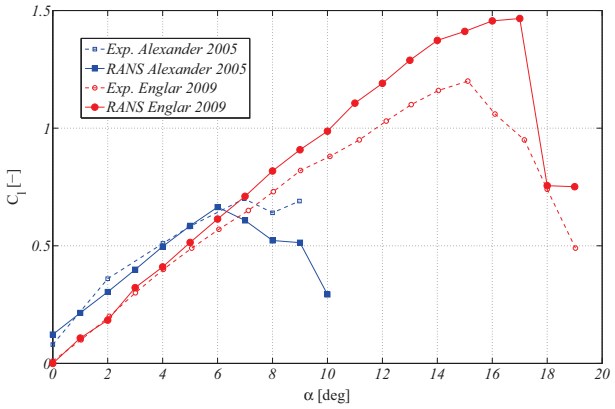

Fig. 6. Numerical lift results for unblown aerofoil from studied references [37][21]

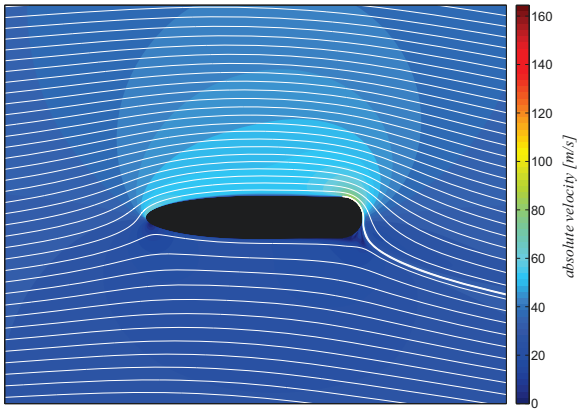

Fig. 7. Absolute velocity flow field from RANS calculations at $\frac{V_{jet}}{V_\infty} = 4.3, \alpha = -2°$

boundary layer or separation control due to entrainment of the flow from the upper surface. The velocity difference between the Coandă jet and the local stream generates a favourable pressure gradient and prevents trailing edge separation. This yields a near inviscid pressure distribution characteristic as it is described by potential theory except minor deviations at the trailing edge suction peak [40]. The imaginary aft stagnation point defines the Kutta condition and is directly affected by the location of jet detachment from the Coandă surface. Indeed, sectional lift coefficients approaching the theoretical inviscid maximum of $2\pi\left(1+\frac{t}{c}\right)$ have been demonstrated [41]. The prevention of separation at the trailing edge leads to a significant drag reduction compared to the baseline aerofoil performance and usually outstrips the bare jet thrust effect. Moreover the suction peaks at the trailing edge annihilate the usual unfavourable adverse pressure gradient in the rear chord fractions and turbulent boundary layer thickening is alleviated. At higher blowing rates the separation control evolves to the so-called super-circulation [18]. A large stagnation point movement leads to a greater circulation than that obtained solely by entraining the boundary layer. Both the forward and aft stagnation point are shifted such that the aerofoil experiences an increase in effective camber and in associated lift even at angles of attack below zero (Fig.7). As already mentioned this high lift generation leads to significant three-dimensional effects inside the wind tunnel and had to be taken into account for validating calculations by reducing the effective angle of attack by $\Delta\alpha = -2°$. Here own calculations could qualitatively reproduce the wind tunnel pressure distribution (Fig.8) even though the jet outflow velocity had to be reduced compared to the given C_μ- value. Englar et al. made similar experiences and gave possible reasons for this discrepancy. Varying total pressure losses due to viscosity effects inside the internal ducts as well as differing slot heights at the jet exit due to non-uniform bending loads influence the local outflow velocity and mass flow rate. Thus, the real flow momentum coefficient may vary from the total value at the section where the pressure sensors are installed. Therefore the integral quantity C_μ may be insufficient information for the purpose of CFD validation because of possible non-uniform blowing across the entire aerofoil span [35]. Moreover the total C_μ- value is typically defined from experiment based on total mass flow rate and jet exit velocities derived from isentropic flow assumption. So it is prone to errors resulting from local total pressure ratios that differ from the free stream value.

Nevertheless the numerically predicted lift generation performance should lie inside acceptable margins despite numerous uncertainties. Fig.9 shows the lift increment for two slot height adjustments predicted by RANS calculations in comparison to the wind tunnel data from reference Englar et al. [21]. The results for the smaller slot size exhibit poor agreement with wind tunnel data even if the curve slope $\frac{\partial \Delta C_L}{\partial C_\mu}$, i.e. lift augmentation, seems to be roughly representative in the respective jet momentum regions. The wind tunnel measurements for the small slot size indicate the existence of a minimum jet momentum that has to

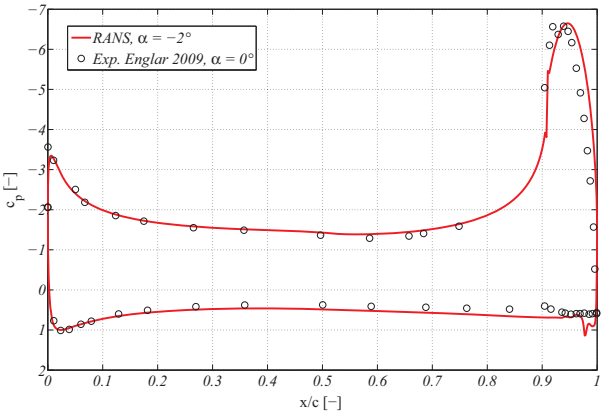

Fig. 8. RANS c_p- results for aerofoil from ref. [21] at $\frac{V_{jet}}{V_\infty} = 4.3$

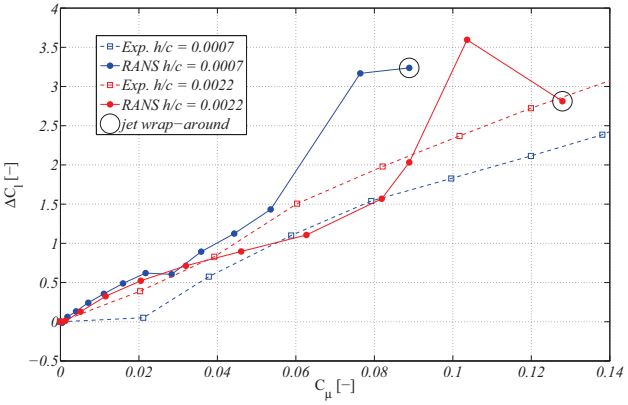

Fig. 9. ΔC_l - comparison of RANS results with experimental data from Englar et al. [21] for different slot heights at $\alpha = 0°$

be passed before the onset of additional lift generation starts. Since this behaviour appears to be less pronounced for larger slot heights the results give reason to assume that small scale viscous effects in the slot exit area are not sufficiently represented by the grid. The numerical results for the larger slot height show reasonable agreement at low outflow velocities but then visibly fall off before they suddenly rise and overestimate the generated lift. The latter behaviour is also experienced in references treating the same flow problem [21, 35] and illustrates once more the challenges to predict correctly the jet flow behaviour on the Coandă surface by RANS calculations. Especially the non-physical jet wrap around phenomenon raises questions addressing numerical stability. As can be seen in Fig.11 at high jet-to-free-stream-velocity-ratios $\frac{V_{jet}}{V_\infty}$ the jet remains attached to the Coandă surface, wraps around and shifts the rear stagnation point to the lower side of the aerofoil. The respective points are marked by black rings in Fig.9 and generally entail a significant lift loss after a preceding peak.

The numerical results for reference Alexander et al. [37] are characterised by a similar behaviour of the lift increment curve (Fig.10). Note that the angle of attack for the RANS calculations had been reduced to $\alpha = 0°$ in order to reduce the uncertainties due to leading edge separation bubbles. The wind tunnel data was only available for $\alpha = 6°$ where separation effects are supposed to have their onset already at moderate blowing rates. In the low jet momentum regions the RANS model results show good agreement with the wind tunnel data while the lift curve slope

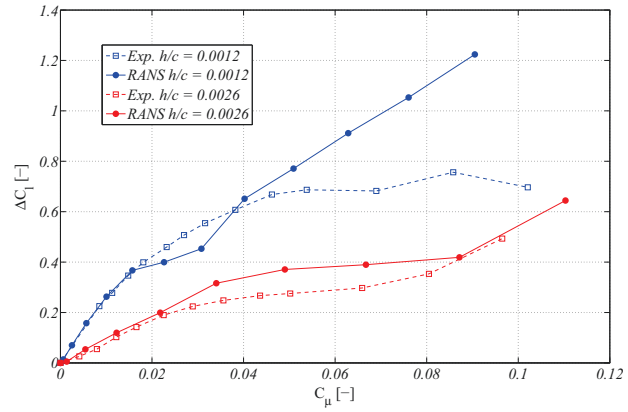

Fig. 10. ΔC_l - comparison of RANS results with experimental data from Alexander et al. [37] for different slot heights at $\alpha = 0°$ (RANS) and at $\alpha = 6°$ (Exp.)

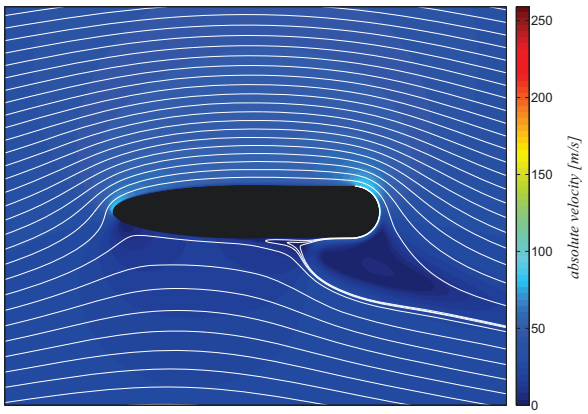

Fig. 11. RANS velocity flow field and stream lines illustrate the jet wrap around phenomenon at $\frac{V_{jet}}{V_\infty} = 7.7$, $\alpha = 0°$

for the smaller slot size exhibits a slight decrease at moderate outflow rates. The discrepancy at high blowing rates is supposed to arise from real flow separations at the leading edge as well as at the trailing edge of the wind tunnel model. When the jet has become supersonic compressible effects have to be expected on the Coandă surface which may lead to expansion wave induced jet detachment [42, 18, 43, 37]. However, the lift increase due to blowing through the larger slot seems to be predicted fairly well despite some overestimation at moderate blowing rates. Summarising own calculation campaigns and literature reviews the experience has been made that large trailing edge radii and small slot heights hold particularly challenging difficulties for RANS modelling activities. While smaller Coandă surface radii are preferable for technical applications due to pressure drag issues, unfortunately small slot sizes still retain their appeal as they promise a significant reduction in pressurised mass flow demand. As the supply of pressurised air flow is crucial for final evaluation of this concept for novel flight control effectors the modelling of thin wall jet sheet layers stay an important research topic in order to increase modelling accuracy and robustness.

3.3.3 Dual-Slot-Blowing

The concept of a steady blown double-slot aerofoil configuration introduces an important difference in nature of the posed flow problem. Except the case where one slot is completely closed, the two opposing jets at the trailing edge define a convection dominated problem which can be solved by RANS calculations more accurately. The following test case is based on the concept of a circulation control aerofoil whose upper and lower slot both are supplied by one plenum chamber imposing one total pressure value. Except viscous effects for very thin slots the maximum outflow velocities of both slots are supposed to be approximately identical regardless of the respective slot height. During the first studies a NACA64A012 aerofoil was modelled having a relative Coandă radius $\frac{r}{c}$ of 1.5% and a total slot height $h_{total} = h_{upper} + h_{lower}$ of $1mm$. Within the scope of the SAGITTA demonstrator the environmental conditions were set to cruise flight conditions at $60\frac{m}{s}$ near ground which result in a Reynold's number of approx. $4 \cdot 10^6$. Fig.13 shows the generated lift force due to double-slot-blowing depending on the outflow momentum ratio η. It is defined as

$$\eta = \frac{(C_\mu)_{upper} - (C_\mu)_{lower}}{(C_\mu)_{upper} + (C_\mu)_{lower}} \approx \frac{h_{upper} - h_{lower}}{h_{total}} \qquad (4)$$

and spans the operational range from the cases of completely closed upper slot ($h_{lower} = h_{total}; \eta = -1$) to completely closed lower slot ($h_{upper} = h_{total}; \eta = 1$). Initially, the lift force exhibits an approximately linear behaviour w.r.t. the control parameter η which illustrates the similarity to conventional plain flap systems. When the upper slot clearly dominates the determination of the rear stagnation point the lift increment grows more than proportionally at higher η-values. However, close to the border case of completely closed lower slot the lift generation seems to exhibit some erratic characteristics. Even if no decelerated convergence behaviour could be identified this unsteadiness does not necessarily arise from physics but can have numerical reasons. In addition, the model showed irregularities for low outflow velocities when both upper and lower slot had almost the same height. The interaction of the jets does not seem to be well defined when diffusive viscous effects get more important than the bare jet momentum ratio which drives the convective portion inside the governing momentum equations. Except some regions near the borderlines the lift increase due to dual-slot-blowing was found to be principally steady and did not exhibit significant instabilities for the studied example. The trend of lift generation dependent on the outflow momentum ratio η gives hope for the successful technical application and encourages the exploration of the concept's design space including its manifold parameters. The integration of the aerodynamic data model into the aircraft model will enable a final statement about the applicability of a double-slotted circulation control aerofoil shape for flight control purposes.

4 CONCLUSION

An introductory literature review covered both integral methods combined with potential theory and computational fluid dynamics mainly represented by RANS approaches. It concluded that the accurate modelling of circulation aerofoils with blown Coandă trailing edges is still an open field of investigation. Current methods are not capable yet to predict the

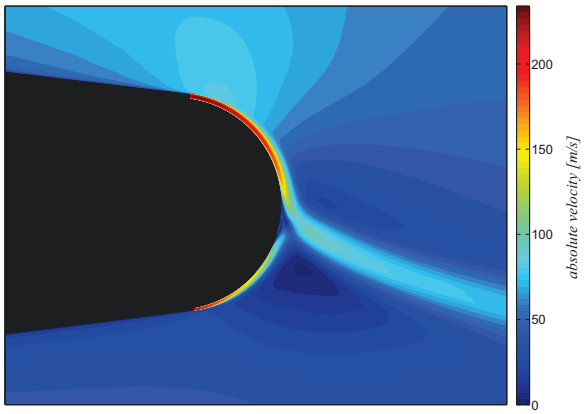

Fig. 12. Trailing edge flow field of dual slot blowing at $\eta = 0.39$, $\frac{V_{jet}}{V_\infty} = 3.5$, $\alpha = 0°$

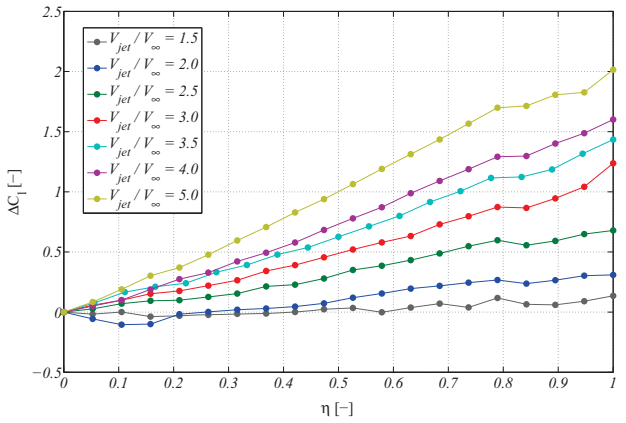

Fig. 13. Lift force reaction of dual slot blowing and varied upper-to-lower-jet-ratio η at $\alpha = 0°$

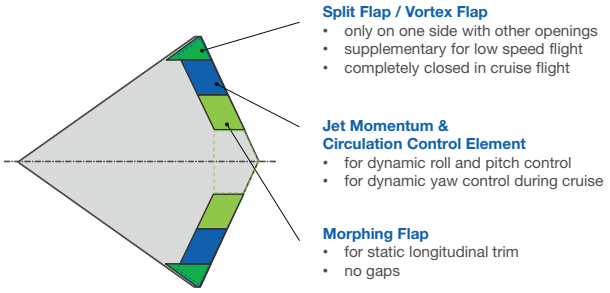

Fig. 14. Illustration of proposed flight control system

aerodynamic forces and moments reasonably correctly throughout the entire range of possible blowing rates. Own research efforts comprised the implementation of a MATLAB tool whose environment provides an incompressible 2D RANS solver including Menter's k-ω-SST-model and Hellsten's stream line curvature correction. After a short description of the tool's main features the flow problem and its setup is specified and builds the basis of the performed numerical studies on lift generation. Two wind tunnel reference cases are modelled and calculated inside the MATLAB environment. Results for the unblown circulation control aerofoils showed reasonable agreement except at high angles of attack where for one case lift was overestimated near stall. Comparing calculations with jet outflow through the upper slot confirmed many of the uncertainties and difficulties found in literature when the RANS method is applied to model the diffusion-driven Coandă jet problem. While lift increments through trailing edge blowing agree sufficiently well for preliminary design purposes at low blowing rates the results show significant difference for high blowing rates in the super-circulation region. A sudden rise in lift generation due to delayed jet detachment up to complete jet wrap around revealed an instability in the RANS modelling method that has also been experienced in similar forms in literature. However, first calculations with dual-slot-blowing showed higher stability in terms of lift curve divergence up to slot adjustments close to the border case of single-slot-blowing. Here, last results encourage the exploration of the system's design space with subsequent performance evaluation within the application on a low aspect ratio flying wing configuration.

5 OUTLOOK

Once having set up a database of aerofoil section moment and force reactions (c_l, c_d, c_m) the aerodynamic performance of the entire wing can be obtained by application of potential theory. The introduction of propulsion and duct system modelling enables conclusions about feasibility and design aspects of the investigated flow control concept. The proposed flight control system layout (Fig.14) will presumably consist of a combination of novel technologies which are topics

of today's research activities inside the framework of the SAGITTA program. Herein, static longitudinal trim is provided by morphing flaps [44] or conventional flap mechanisms whose squatter prone gaps are covered by elastic radar beam absorbing materials [45]. Generally slow flap deflection dynamics for longitudinal trim alleviate the deflection rate requirements for morphing structures. Sufficient stiffness can be obtained without excessive actuator weight and power consumption. Since the envisaged flying wing configuration without vertical surfaces is intentionally designed statically unstable around the yaw axis crosswind landing is critical. Therefore unconventional split flaps based on vortex generation at the most outboard position shall help to overcome the increased yaw control authority requirements at low speeds when engine thrust settings and bleed air supply are low as well. In order to maintain one clean shell without surface interruptions for low-observability reasons the vortex flaps are limited to asymmetric implementation w.r.t. the xy-plane, i.e. only on the half shell already containing all other openings. For highly dynamic control manoeuvres fluidic circulation control effectors as presented in this study provide the required control moments. This concept is also suitable for yaw control when air flow momentum is controlled differentially on the wing half spans. The high mass flow demands during this control mode could be met during cruise flight when the engines are operating at high power settings. For evaluations of transonic cruise flight an aerodynamic data set will be necessary that implies compressibility effects. Therefore the existing MATLAB tool shall be enhanced to enable compressible calculations. Suction peaks at the trailing edge through double-slot-blowing for drag reduction purposes are supposed to have an interesting effect on the transsonic shock position including the aft boundary layer.

References

[1] K. Stadlberger and M. Hornung. Design Drivers for Novel Flight Control Effectors for Low Aspect Ratio Flying-Wing Configurations. In *Proceedings DGLR Congress 2012*, 2012.

[2] R. Imber and E. Rogers. Investigation of a circular planform wing with tangential fluid ejection. In *34th Aerospace Sciences Meeting and Exhibit*, Aerospace Sciences Meetings. American Institute of Aeronautics and Astronautics, 1996.

[3] E. Rogers and M. Donnelly. Characteristics of a Dual-Slotted Circulation Control Wing of Low Aspect Ratio Intended for Naval Hydrodynamic Applications. In *42nd AIAA Aerospace Sciences Meeting and Exhibit*, Aerospace Sciences Meetings. American Institute of Aeronautics and Astronautics, 2004.

[4] C. Harley, P. Wilde, and W. Crowther. Application of Circulation Control manoeuvre effectors for three axis control of a tailless flight vehicle. In *47th AIAA Aerospace Sciences Meeting including The New Horizons Forum and Aerospace Exposition*, Aerospace Sciences Meetings. American Institute of Aeronautics and Astronautics, 2009.

[5] J. Dunham. A theory of circulation control by slot-blowing, applied to a circular cylinder. *Journal of Fluid Mechanics*, 33(03):495–514, 1968.

[6] E. S. Levinsky and T. T. Yeh. Analytical and experimental investigation of circulation control by means of a turbulent Coanda jet, 1972.

[7] F. A. Dvorak and R. J. Kind. Analysis Method for Viscous Flow over Circulation-Controlled Airfoils. *Journal of Aircraft*, 16(1):23–28, 1979.

[8] F. A. Dvorak. Calculation of turbulent boundary layers and wall jets over curved surfaces. *AIAA Journal*, 11(4):517–524, 1973.

[9] F. A. Dvorak and D. H. Choi. Analysis of circulation-controlled airfoils in transonic flow. *Journal of Aircraft*, 20(4):331–337, 1983.

[10] F. Dvorak, D. Strash, B. York, and S. Dash. Improved algorithms for circulation-control airfoils in transonic flow. In *25th AIAA Aerospace Sciences Meeting*, Aerospace Sciences Meetings. American Institute of Aeronautics and Astronautics, 1987.

[11] C. Novak and K. Cornelius. An LDV investigation of a circulation control airfoil flowfield. In *24th Aerospace Sciences Meeting*, Aerospace Sciences Meetings. American Institute of Aeronautics and Astronautics, 1986.

[12] H. F. Fasel, A. Gross, and S. Wernz. Investigation of Turbulent Coanda Wall Jets Using DNS and RANS. In *Applications of Circulation Control Technology*, Progress in Astronautics and Aeronautics, pages 401–420. American Institute of Aeronautics and Astronautics, 2006.

[13] R. C. Swanson, C. L. Rumsey, and S. G. Anders. Aspects of Numerical Simulation of Circulation Control Airfoils. In *Applications of Circulation Control Technology*, Progress in Astronautics and Aeronautics, pages 469–498. American Institute of Aeronautics and Astronautics, 2006.

[14] A. Zacharos and K. Kontis. Numerical Studies on an Active Flow Circulation Controlled Flap Concept for Aeronautical Applications. *Transactions of the Japan Society for Aeronautical and Space Sciences*, 49(163):25–30, 2006.

[15] P. A. Chang, J. Slomski, T. Marino, M. P. Ebert, and J. Abramson. Full Reynolds-Stress Modeling of Circulation Control Airfoils. In *Applications of Circulation Control Technology*, Progress in Astronautics and Aeronautics, pages 445–468. American Institute of Aeronautics and Astronautics, 2006.

[16] R. C. Swanson and C. L. Rumsey. Computation of circulation control airfoil flows. *Computers & Fluids*, 38(10):1925–1942, 2009.

[17] W. Baker and E. Paterson. RANS CFD Simulation of a Circulation-Control Foil: Validation of Performance, Flow Feild, and Wall Jet. In *3rd AIAA Flow Control Conference*, Fluid Dynamics and Co-located Conferences. American Institute of Aeronautics and Astronautics, 2006.

[18] R. J. Englar. Two-Dimensional Subsonic Wind Tunnel Tests of Two 15-Percent Thick Circulation Control Airfoils, 1971.

[19] R. Swanson, C. Rumsey, and S. Anders. Progress Towards Computational Method for Circulation Control Airfoils. In *43rd AIAA Aerospace Sciences Meeting and Exhibit*, Aerospace Sciences Meetings. American Institute of Aeronautics and Astronautics, 2005.

[20] F. K. Owen and A. K. Owen. Measurement and Analysis of Circulation Control Airfoils. In *Applications of Circulation Control Technology*, Progress in Astronautics and Aeronautics, pages 105–112. American Institute of Aeronautics and Astronautics, 2006.

[21] R. Englar, G. JONES, B. Allan, and J. Lin. 2-D Circulation Control Airfoil Benchmark Experiments Intended for CFD Code Validation. In *47th AIAA Aerospace Sciences Meeting including The New Horizons Forum and Aerospace Exposition*, Aerospace Sciences Meetings. American Institute of Aeronautics and Astronautics, 2009.

[22] T. Nishino and K. Shariff. Numerical Study of Wind-Tunnel Sidewall Effects on Circulation Control Airfoil Flows. *AIAA Journal*, 48(9):2123–2132, 2010.

[23] B. E. Launder and W. Rodi. The Turbulent Wall Jet Measurements and Modeling. *Annu. Rev. Fluid Mech.*, 15(1):429–459, 1983.

[24] P. Pajayakrit and R. J. Kind. Assessment and Modification of Two-Equation Turbulence Models. *AIAA Journal*, 38(6):955–963, 2000.

[25] A. Hellsten. Some improvements in Menter's k-omega SST turbulence model. In *29th AIAA, Fluid Dynamics Conference*, Fluid Dynamics and Co-located Conferences. American Institute of Aeronautics and Astronautics, 1998.

[26] M. L. Shur, M. K. Strelets, A. K. Travin, and P. R. Spalart. Turbulence Modeling in Rotating and Curved Channels: Assessing the Spalart-Shur Correction. *AIAA Journal*, 38(5):784–792, 2000.

[27] C. L. Rumsey and T. Nishino. Numerical study comparing RANS and LES approaches on a circulation control airfoil. *International Journal of Heat and Fluid Flow*, 32(5):847–864, 2011.

[28] B.-Y. Min, W. Lee, R. Englar, and L. N. Sankar. Numerical Investigation of Circulation Control Airfoils. *Journal of Aircraft*, 46(4):1403–1410, 2009.

[29] T. Nishino and K. Shariff. Effect of Jet Nozzle Lip Momentum Loss on Circulation Control Airfoil Performance. *AIAA Journal*, 50(3):551–558, 2012.

[30] T. Nishino, S. Hahn, and K. Shariff. Calculation of the Turbulence Characteristics of Flow Around a Circulation Control Airfoil Using LES (Invited Paper). In *48th AIAA Aerospace Sciences Meeting Including the New Horizons Forum and Aerospace Exposition*, Aerospace Sciences Meetings. American Institute of Aeronautics and Astronautics, 2010.

[31] N. Madavan and M. Rogers. Direct Numerical Simulation of Flow Around a Circulation Control Airfoil. In *5th Flow Control Conference*, Fluid Dynamics and Co-located Conferences. American Institute of Aeronautics and Astronautics, 2010.

[32] D. B. Spalding. A novel finite difference formulation for differential expressions involving both first and second derivatives. *International Journal for Numerical Methods in Engineering*, 4(4):551–559, 1972.

[33] F. H. Harlow and J. E. Welch. Numerical Calculation of Time–Dependent Viscous Incompressible Flow of Fluid with Free Surface. *Physics of Fluids (1958-1988)*, 8(12):2182–2189, 1965.

[34] F. R. Menter, M. Kuntz, and R. Langtry. Ten Years of Industrial Experience with the SST Turbulence Model. *Turbulence, Heat and Mass Transfer*, (4):625–632, 2003.

[35] B. Allan, G. Jones, and J. Lin. Reynolds-Averaged Navier-Stokes Simulation of a 2-D Circulation Control Wind Tunnel Experiment. In *49th AIAA Aerospace Sciences Meeting including the New Horizons Forum and Aerospace Exposition*, Aerospace Sciences Meetings. American Institute of Aeronautics and Astronautics, 2011.

[36] C. Rumsey and T. Nishino. Numerical Study Comparing RANS and LES Approaches on a Circulation Control Airfoil. In *49th AIAA Aerospace Sciences Meeting including the New Horizons Forum and Aerospace Exposition*, Aerospace Sciences Meetings. American Institute of Aeronautics and Astronautics, 2011.

[37] M. G. Alexander, S. G. Anders, S. K. Johnson, J. P. Florance, and D. F. Keller. Trailing Edge Blowing on a Two-Dimensional Six-Percent Thick Elliptical Circulation Control Airfoil Up to Transonic Conditions: NASA/TM-2005-213545, 2005.

[38] K. Kwon and S. O. Park. Aerodynamic Characteristics of an Elliptic Airfoil at Low Reynolds Number. *Journal of Aircraft*, 42(6):1642–1644, 2005.

[39] S. F. Hoerner and H. V. Borst. *Fluid-Dynamic Lift: practical information on aerodynamic and hydrodynamic lift*. Hoerner Fluid Dynamics, Alburquerque and N.M, 2 edition, 1985.

[40] R. M. Williams and H. J. Howe. Two Dimensional Subsonic Wind Tunnel Tests on a 20 Percent Thick, 5 Percent Cambered Circulation Control Airfoil, 1970.

[41] N. J. Wood and J. N. Nielsen. Circulation control airfoils as applied to rotary-wing aircraft. *Journal of Aircraft*, 23(12):865–875, 1986.

[42] R. J. Englar. Two-Dimensional Transonic Wind Tunnel Tests of Three 15-Percent Thick Circulation Control Airfoils, 1970.

[43] R. J. Englar. Experimental Investigation of the High Velocity Coanda Wall Jet Applied to Bluff Trailing Edge Circulation Control Airfoils, 1975.

[44] B. Gramüller, J. Boblenz, and C. Hühne. PACS - Realization of an Adaptive Concept Using Pressure Actuated Cellular Structures. In *63. Deutscher Luft- und Raumfahrtkongress der Deutschen Gesellschaft für Luft- und Raumfahrt e.V.*, 2014.

[45] L. da Rocha-Schmidt and H. Baier. Morphing Skins and Gap Covers for Aerodynamic Control Surfaces. In *62. Deutscher Luft- und Raumfahrtkongress der Deutschen Gesellschaft für Luft- und Raumfahrt e.V.*, 2013.